PSK to CSK Mapping for Hybrid Systems Involving the Radio Frequency and the Visible Spectrum

Alain Richard Ndjiongue, Thokozani Shongwe, H. C. Ferreira, Telex Ngatched and A. J. Han Vinck

Abstract—This paper presents an efficient technique to map phase shift keying (PSK) signalling to colour shift keying (CSK) constellation, to establish a full link in hybrid systems involving the radio frequency (RF) and the visible spectrum. It fits in systems combining (first link) wireless communication technologies such as the wireless fidelity (WiFi) or wired communication technologies such as power line communications (PLC) to visible light communications (VLC) technology (second link). On the first link, PSK technique is used to convey the information, while, on the second link, a technique based on colour variation is deployed. WiFi standards targeted are those that employ PSK as sub-carrier modulation techniques (IEEE 802.11a/11g/11n). The PSK complex constellation observed at the output of the first link is converted into colours using the hue-saturation-value/intensity (HSV/I) colour models. The constant lighting required in VLC corresponds with the coordinate I of the HSI and the colour constraint is met by assigning adequate current intensities to the red-green-blue LEDs (RGB-LEDs) used. The design meets the requirements of CSK constellation design outlined in IEEE 802.15.7. The performance of the system is analysed through bit error rate curves obtained by simulations, for binary PSK (BPSK) and quadrature PSK (QPSK), 8PSK and 16PSK constellations. The results show that as the constellation size increases, the performance of the system decreases.

Index Terms—PSK-CSK, Visible light communications, Hybrid RF-VLC systems, CSK constellation design, HSI colour family, Complex vectors to colour mapping.

I. INTRODUCTION

THIS demo file is intended to serve as a "starter Research in visible light communication (VLC) technology has been advanced in the last couple of years. In VLC, light emitting diodes (LEDs) are used to couple the message signal to the channel. LEDs are generally made for lighting purposes. Nowadays, they serve two different applications, namely lighting and communication. The advantages offered by their dual use can never be over-emphasised: on the one hand, it offers economic advantages due to the omnipresence of light bulbs, on the other, the bandwidth offered by the visible spectrum is large enough to accommodate very high data rate communication applications. White LEDs are mostly used in VLC to transmit data by modulating the intensity of their forward currents. A specific class of LEDs, including multiple colour-LEDs in one package, is used in systems exploiting colour variation for data transmission, such as colour shift keying (CSK). Red-green-blue LEDs (RGB-LEDs) are the most used colour-LEDs. This class of LED is capable of producing the maximum of colours of the visible spectrum. They are therefore very solicited in VLC, especially in modulations in which the colour variation is used to convey the information. CSK is one of those modulation techniques in which the

multi-wavelength of the RGB-LEDs is used to transmit data [1], corresponding with PHY III proposed in IEEE 802.15.7 standards [1], [2].

The applications of VLC are multiple. Some of them are hybrid systems involving the radio frequency (RF) and the visible spectrum: VLC can be used to release the RF spectrum in wireless fidelity (WiFi) [3], it can also be used to efficiently connect the power line communication (PLC) technology end user. Hybrid systems combining RF and the visible spectrum are available in the literature. Here we present some examples: In [4], the performance of hybrid RF-VLC system is analysed in terms of its throughput and fairness in diverse down-link cell formation scenarios. In [5] and [6], hybrid system combining power line communications PLC and VLC is proposed using orthogonal frequency division multiplexing (OFDM). An integrated system of white LEDs VLC and PLC using a single carrier binary PSK (BPSK) is proposed in [7]. A PLC-VLC cascaded channel is studied and presented in [8] using OFDM on the PLC channel and VLC over the VLC channel. The result shows that in cascaded channels, the performance of the system is imposed by the bad channel. [9] and [10] investigate a system using binary frequency shift keying (BFSK) on the PLC link and on-off keying (OOK) on the VLC link. [9] presents a practical implementation of the hybrid PLC-VLC system using BFSK and OOK while [10] looks at the semi-hidden Markov model of the same system. It proposes a Semi-hidden Markov modeling of a low complexity FSK-OOK in-house PLC and VLC integration. A hybrid radio frequency and broadcast VLC system integrating WiFi and VLC is proposed in [11]. A combination of the CSK scheme and pulse position modulation (PPM) is analysed in [12], while [13] proposes to combine CSK and complementary pulse position modulation (CPPM).

In this paper, we propose an efficient technique that will be used in hybrid systems combining RF and the visible spectrum. The RF signal is modulated using the PSK modulation method and the optical part uses a multi-wavelength technique to convey the information. We analyse the performances of hybrid modulations combining PSK and CSK. The CSK constellation is designed based on the hue-saturation-intensity (HSI) colour family. The colour wheel method is exploited to map the incoming PSK complex symbols to colours. An important advantage offered by the HSI colour family is the constant intensity (I) of the brightness. The hue-saturation-value/intensity (HSV/I) cone is inserted into the RGB cube to match the intensities needed to produce the colours. An arbitrary value is attributed to an internal parameter x, which is proportional to the modulus of the PSK complex symbol

detected. The parameter x is used to control the brightness (x can be tuned to give optimal lighting), and different values of x result in different bit error rate performances (x can be tuned to give optimal communication performance). The best trade-off between communication and lighting is obtained for a set of values attributed to x, corresponding to an average value of 85.33% of V and S. The proposed technique provides two important advantages: easy conversion from PSK complex symbols to colours and strict constant power envelope within the transmission set in CSK, respecting the average colour required. The results show that as the PSK constellation size increases, the performance of the system decreases. Nevertheless, in any case, a trade-off is found between lighting and communication. The applications of the proposed technique fall in hybrid systems including the RF and visible spectrums. They must all use the PSK technique over the first link of the hybrid system and CSK over the second. These applications include wireless to wireless systems such as WiFi to light fidelity (LiFi), and wired to wireless systems such as PLC-VLC systems.

The remainder of this paper is organised as follows: in Section II, the CSK constellation design is presented. In Section III, we describe the HSV/I colour space and present the technique used to convert PSK complex symbols to colours. The proposed mapping method is detailed in Section IV. We describe the mapping method and provide constellation diagrams, the Euclidean distances for BPSK, QPSK, 8PSK and 16PSK constellations, and the error probability. Simulation model and results are presented in Section V, and the paper is concluded in Section VI.

II. CSK CONSTELLATION DESIGN

The CSK modulation technique is used to map symbols to colours. In this scheme, each symbol is mapped to a colour and the colour constellation fits in a triangle made of the three primary colours red, green and blue. Afterwards, the resulting colour obtained must be produced with a constant power envelope as presented in [14], [15]. Some CSK design examples can be found in the literature: in [14], a design of the CSK constellation is presented using a billiard algorithm, and the performance of the system is analysed through simulation. A different approach is proposed in [16], where the CSK constellation is designed and implemented using the interior point method. In [17], an analysis of the design of CSK constellation for VLC technology is proposed. A prototype is also proposed to validate the performance of the system. Deep analysis of the CSK scheme is proposed in [15]. It investigates multiple possibilities, it takes into account multiple groups of LEDs having more than three LEDs per group. The model is validated by a comparative implementation for 8 and 16-CSK.

A. Standardised CSK Constellation Design

CSK is outlined in IEEE 802.15.7 standard [1]. The constellation triangle and throughput requirements are described. The transmission set fits in the triangle (R, G, B) presented in Fig 1, where R, G and B are the primary red, green and blue colours, respectively, and bounded by 0 and 1. Let $\{s_1, s_2, \ldots, s_N\}$ be
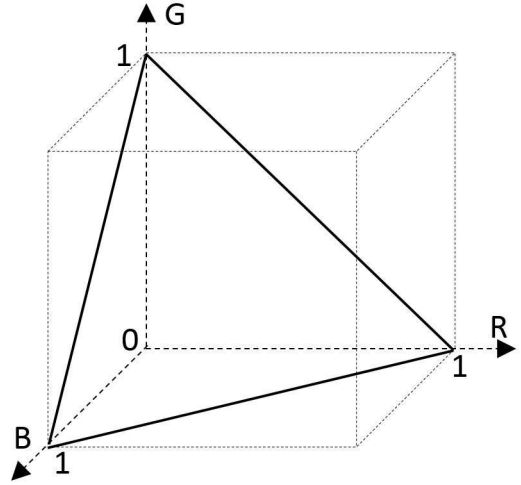

Figure 1. Transmission set and decision region.

the incoming symbol set to be mapped to colours, N being the constellation size. The set is transmitted by mapping the kth symbol S_k ($k = 1, 2, \ldots, N$), to the intensities of the red, green and blue LEDs to produce the kth colour. The average optical power (P^{avg}) must remain constant within the transmitted symbols set. Definitions of the average power, the average luminous flux and the average colour are provided in the Appendix. The transmission in a channel affected by white Gaussian noise is governed by

$$\tilde{\mathbf{s}}_i = \mathbf{H}\mathbf{s}_i + \mathbf{n}_i, \tag{1}$$

where $\tilde{\mathbf{s}}_i$ and $\mathbf{s}_i$ are the received and the transmitted symbol sets, respectively. $\mathbf{n}_i$ the noise vector and $\mathbf{H}$ the channel frequency response. $\mathbf{H}$ is a 3×3 matrix whose diagonal part represents the gains between the LED current and the corresponding photodetector (PD) current, and the rest of the entries represent the crosstalk gains between single channels. $\mathbf{H}$ is given by

$$\mathbf{H} = \left[\begin{array}{ccc} h_{\mathbf{rr}} & h_{rg} & h_{rb} \\ h_{gr} & h_{\mathbf{gg}} & h_{gb} \\ h_{br} & h_{bg} & h_{\mathbf{bb}} \end{array} \right]. \tag{2}$$

III. THE HSI COLOUR FAMILY AND COMPLEX NUMBERS

A. The HSI colour family

The hue-saturation-intensity (HSI) colour family groups the HSI, HSV and the hue-saturation-lightness (HSL) colour models. They are all based on the human visual system and use cylindrical coordinates to represent a colour. The use of the HSI colour family is motivated by the fact that the I (V, L) components can easily be separated from the other parameters (H and S). H is an attribute defining the purity of the colour, while S defines the degree of dilution of a pure colour into a white light. I (V, L) gives the brightness of the indicated colour. HSI, HSV and HSL models are similar in H and S coordinates, but are different on the values of I, V and L.

B. HSV and HSI colour models

HSV/I is a mathematical representation of colours in three cylindrical-coordinates H, S and V/I [18]. H represents the colour shade and is mathematically an angle between 0° and 360°. S and V, both bounded by 0 and 1 define the purity of the colour and its brightness, respectively. In HSV colour space as in any model of the HSI family, the colour is described almost in the same manner as the human eyes [19], while the colour information such as chroma, brightness, saturation and hue can easily be separated. Originally, the HSV colour space is represented by a hex-cone, having six lateral faces and one top-face. The lateral faces join on the black colour. The white colour represents the centre of the top-face of the hex-cone and the cone axis is the black-white line. The minimum distance between the axis and the edge of the cone represents the saturation of the colour. Gradually, as one moves away from the black colour, one gains in brightness and saturation. HSV is widely used in applications involving object detection and recognition, and in image analysis.

C. Representation of complex symbols in colours

To convert the incoming complex symbols to colours, we apply the colour wheel of complex functions. The colour wheel is a representation of complex numbers using colours [20], [21]. It works in the HSV/I colour space. The argument of the complex number corresponds to the hue (H), its modulus corresponds to the values V and S. In general, this method maps the complex set C to the HSV colour space in such a way that each point $a + jb$ of the complex space is associated with the colour code $HSV(a + jb)$. This is materialised by

$$HSV(a+jb) : \begin{cases} H = arg[a+jb] & \text{(a)}, \\ S = 0.5 + 0.5sin(2\pi r) & \text{(b)}, \\ V = 0.5 + 0.5cos(2\pi r) & \text{(c)}, \end{cases} \quad (3)$$

where $r = log[1 + |a + jb|]$ is the radius of the wheel. A description of the colour wheel technique is shown in Fig. 2. The origin of the system is chosen in such a way that +1 (0°) and -1 (180°) are assigned to red and cyan colours, respectively. The colours are organised by rotation of the wheel. The argument of the complex number (3-a) gives the position of the colour on the wheel. Brightness (intensity) and saturation are constants for all complex symbols that have the same modulus.

IV. PSK TO CSK DESIGN TECHNIQUE

The system model is depicted in Fig. 3. The incoming bits are grouped into an M-ary PSK constellation. The PSK complex symbols are then converted into the HSV colour space. Thereafter, the colours are inserted into the unit RGB cube so that the required current intensities are applied to achieve transmission.

A. PSK to CSK Mapping

Let $\mathbf{A} = \{A_1, A_2, \ldots, A_M\}$ be the PSK complex constellation of size M to be mapped to colours. Let $A_k \in \mathbf{A}$ be the kth complex symbol ($k = 1, 2, \ldots, M$). In PSK modulation,
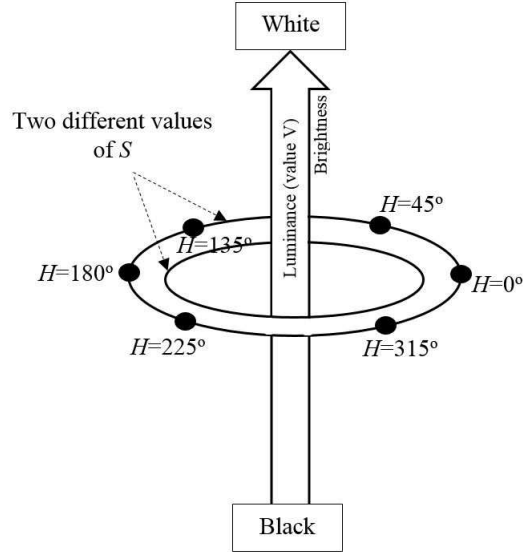

Figure 2. Description of the colour wheel principle used to map complex symbols to colours in HSV colour space.
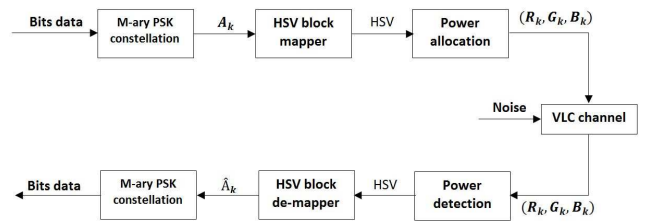

Figure 3. Description of the full transmission in a CSK based HSV colour space.

the information is conveyed by the phase of the complex symbol, not its magnitude. This implies that the magnitude of A_k can be altered without affecting the message conveyed. Let us denote the variation of the magnitude of PSK symbols by $x = \lambda|A_k| = \lambda|a_k + jb_k|$, where $\lambda \in \mathbb{N}$. An example illustrating multiple values of x for a given magnitude $|A_k|$ and phase $(\frac{\pi}{4})$ of the symbol is presented in Fig 4. By exploiting (3), we will later show, in Section V that different values of x (different magnitudes of the complex symbol) result in different performances in the PSK-CSK system proposed in this paper. Afterwards, A_k is converted into the hue H_k, the
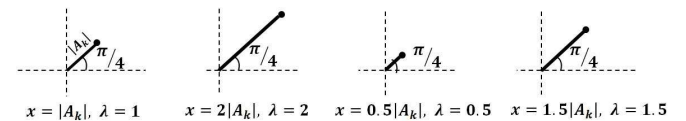

Figure 4. Illustration of the value of x corresponding to a complex magnitude $|A_k|$ for multiple values of λ.

saturation S_k, and the brightness V_k or I_k. This is explained by

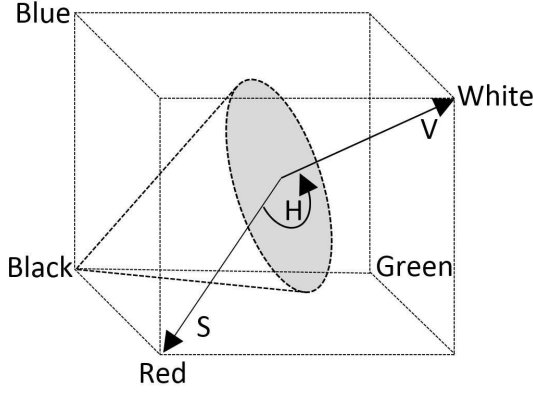$$A_k \longrightarrow (H_k, S_k, V_k/I_k) \longrightarrow (R_k, G_k, B_k), \quad (4)$$

Figure 5. HSV cone built inside the RGB unique cube to link HSV to RGB for lighting pre-compensation.

where H_k, S_k and V_k/I_k are the HSV(I) parameters corresponding to the kth symbol. The parameters R_k, G_k and B_k are the intensities of the red, green and blue LEDs for producing the colour C_k.

B. Intensity requirement and power allocation

The power constraint of VLC technology demands that the constant brightness related to the average luminous flux (see in the Appendix), which is given in (5) for the kth symbol, be constant [22]. Since the brightness produced by a colour is the sum of the brightness produced by the three LEDs used to produce the colour, we have

$$P^{avg} = R_k + G_k + B_k, \qquad (5)$$

where R_k, G_k and B_k are the optical powers (see (4)) produced by the red, green and blue LEDs, respectively. Practically, the design imposes bounds on the luminous flux from which the required power is calculated (see in the Appendix). Consequently, the power related to the kth symbol is bounded as

$$P^{avg} - \Delta P \le P_k \le P^{avg} + \Delta P. \qquad (6)$$

To meet this power requirement, the HSV/I cone is inserted into the RGB unit cube (see Fig. 5) in such a way that the symbols organised on the wheel, are represented by their RGB components whose intensities will always sum up to a value proportional to the power envelope required. Practically, a typical conversion from HSV/I colour space to RGB colour space is needed to match the intensities of the LEDs. The algorithm used to convert the HSV/I parameters to RGB parameters is based on the technique presented in [23] and [24], with S and $V(I)$ being constant for all PSK symbols converted into colours. The RGB coordinates are deduced from some combinations of $V(I)$, S and H as detailed in [23] and [24]. Tables I, II, III and IV give RGB parameters from HSV colour space for BPSK, QPSK, 8PSK and 16PSK incoming complex symbols, respectively, for $V = S = 85.33\%$. The different PSK modulation of different order (BPSK, QPSK, 8PSK, 16PSK) all consider that the coordinates of the colour c_k, (r_k, g_k, b_k) are proportional to the three forward current

intensities i_{rk}, i_{gk}, and i_{bk} of the RGB-LED for producing the colour c_k. Hence, by analogy to (6), the sum of the coordinates of c_k is bounded as

$$\sigma_k^{min} \le \sigma_k \le \sigma_k^{max}, \qquad (7)$$

where $\sigma_k = r_k + g_k + b_k$, and, σ_k^{min} and σ_k^{max} are the lower and the upper boundaries of σ_k, respectively. In this design, we impose $\sigma_k^{min} = 1.1037$ and $\sigma_k^{max} = 1.8318$. The average sum $\sigma^{avg} = 1.4677$ is the same for all constellation sizes. Figs. 6, 7, 8 and 9 show the HSV colour constellation for BPSK, QPSK, 8PSK and 16PSK incoming complex symbols, respectively, built from $V = S = 0.8533$. In each of them: a) shows the wheel and b) shows the PSK-CSK constellation in the RGB cube. The mapping is based on the colour wheel defined by the radius r (saturation S and value V) and the RGB coordinates are calculated based on the HSV to RGB conversion algorithm. This is shown later on the constellations. In each of the figures, the points are situated on an equidistant plate from the black colour in the RGB unit cube, showing the constant brightness between symbols. In fact, the design allows very little error in illumination. For example, in the case of two symbols, the distance between points and the black colour are $d_1 = 0.7595$ and $d_2 = 1.4719$, showing that the equidistant plate is situated at 1.1157 from the black colour. This allows an error ε_d of 0.3562 on the four points given with a standard deviation of 0.1269. In the case of four symbols, the distance between points and the black colour are $d_1 = 0.8715$, $d_2 = 0.9915$, $d_3 = 1.2132$, and $d_4 = 0.9915$, showing that the equidistant plate is situated at 1.0169 from the black. This allows an error ε_d on the four points given by $0.0254 \le \varepsilon_d \le 0.1963$ with a standard deviation of 0.1235. The same analysis shows that for eight symbols, the design makes an error comprised between 0.0411 and 0.1935 with a standard deviation of 0.1251. For 16 symbols, we obtain an error between 0.0305 and 0.2043, and a standard deviation of 0.1033. The errors and standard deviations analysed here explain how constant is the lighting, not the communication performance.

Table I
RGB COORDINATES OF BPSK-HSV INCOMING SYMBOLS FOR $x = 0.1331$.

	H	V = S	r	g	b	r+g+b
s_1	0	0.8533	0.8533	0.1252	0.1252	1.1037
s_2	90	0.8533	0.1252	0.8533	0.8533	1.8318

Table II
RGB COORDINATES OF QPSK-HSV INCOMING SYMBOLS FOR $x = 0.1331$.

	H	V = S	r	g	b	r+g+b
s_1	0	0.8533	0.8533	0.1252	0.1252	1.1037
s_2	90	0.8533	0.4892	0.8533	0.1252	1.4697
s_3	180	0.8533	0.1252	0.8533	0.8533	1.8318
s_4	270	0.8533	0.4892	0.1252	0.8533	1.4677

V. SIMULATION AND RESULTS

We assume perfect conversion between systems: From complex constellations to the HSV/I colour space and vice-versa, and from the HSI colour space to the RGB colour

Table III
RGB COORDINATES OF 8PSK-HSV INCOMING SYMBOLS FOR $x = 0.1331$.

	H	V = S	r	g	b	r+g+b
s_1	0	0.8533	0.8533	0.1252	0.1252	1.1037
s_2	45	0.8533	0.8533	0.6712	0.1252	1.6497
s_3	90	0.8533	0.4892	0.8533	0.1252	1.4677
s_4	135	0.8533	0.1252	0.8533	0.3072	1.2857
s_5	180	0.8533	0.1252	0.8533	0.8533	1.8318
s_6	225	0.8533	0.1252	0.3072	0.8533	1.2857
s_7	270	0.8533	0.4892	0.1252	0.8533	1.4677
s_8	315	0.8533	0.8533	0.1252	0.6712	1.6497

Table IV
RGB COORDINATES OF 16PSK-HSV INCOMING SYMBOLS FOR $x = 0.1331$.

	H	V = S	r	g	b	r+g+b
s_1	0	0.853	0.8533	0.1252	0.1252	1.1037
s_2	22.5	0.853	0.8533	0.3982	0.1252	1.3767
s_3	45	0.853	0.8533	0.6723	0.1252	1.6497
s_4	67.5	0.853	0.7623	0.8533	0.1252	1.7408
s_5	90	0.853	0.4892	0.8533	0.1252	1.4677
s_6	112.5	0.853	0.2162	0.8533	0.1252	1.1947
s_7	135	0.853	0.1252	0.8533	0.3092	1.2857
s_8	157.5	0.853	0.1252	0.8533	0.5803	1.5587
s_9	180	0.853	0.1252	0.8533	0.8533	1.8318
s_{10}	202.5	0.853	0.1252	0.5803	0.8533	1.5587
s_{11}	225	0.853	0.1252	0.3072	0.8533	1.2857
s_{12}	247.5	0.853	0.2162	0.1252	0.8533	1.1949
s_{13}	270	0.853	0.4592	0.1252	0.8533	1.4677
s_{14}	292.5	0.853	0.7623	0.1252	0.8533	1.7408
s_{15}	315	0.853	0.8533	0.1252	0.6723	1.6497
s_{16}	337.5	0.853	0.8533	0.1252	0.3982	1.3767

Figure 6. Representation of BPSK complex constellation in colours for $x = 0.1331$, $V = S = 0.8533$: a) Colour wheel for BPSK and b) the corresponding constellation in the RGB plan.
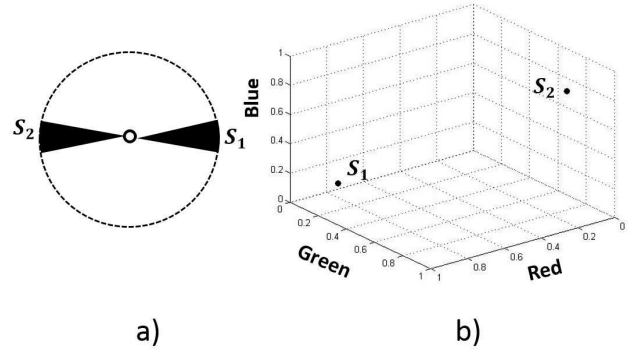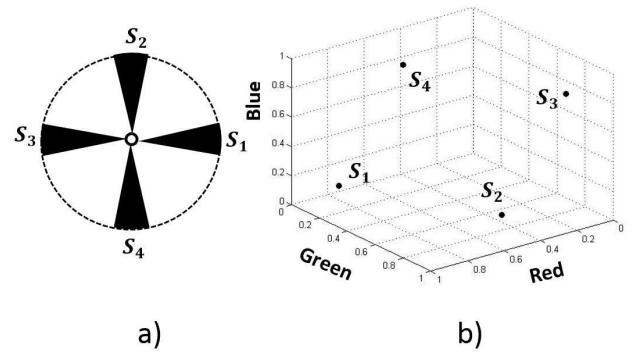

Figure 7. Representation of QPSK complex constellation in colours for $x = 0.1331$, $V = S = 0.8533$: a) Colour wheel for QPSK and b) the corresponding constellation in the RGB plan.

space and vice-versa. When PSK constellations are converted into colours, the kth and $(k + 1)^{th}$ symbols have the same brightness and saturation ($x_k = x_{k+1}$). This means that the distance between c_k and c_{k+1} (k^{th} and $(k + 1)^{th}$ colours, respectively) depends on H_k, which is independent of x_k ($x_k = \lambda|a_k + jb_k|$). In the HSV/I colour space, this distance is given by $d_{HSV} = |H_k - H_{k+1}|$. The optimum distance between two colours is calculated in the RGB colour cube because RGB-LEDs are used to produce the colours. Hence, we base the detection on the RGB colour space. The distance, d_{sr}, between the sent colour, c_k^s, and the received colour, c_k^r, is calculated by applying the Euclidean theorem of distance between c_k^s and c_k^r. The objective is to quantify and minimise the maximum likelihood Euclidean distance between c_k^s and c_k^r. This is achieved by applying the maximum a posteriori probability (MAP) detection rule. Since the transmission is dominated by white Gaussian noise, and the a-priori message probabilities are all equal, the optimum receiver has to minimise the squared Euclidean distance metric target on the point c_k^r [15] (See The Appendix for probabilistic decision and distance optimisation formulas).

A. Distance analysis

To put the Euclidean distance calculation in the RGB space into perspective, we present and discuss the results in Tables V, VI and VII for QPSK-CSK, 8PSK-CSK and 16PSK-CSK, respectively. A look at the constellation of 8PSK-CSK and 16PSK-CSK shows that the minimum distance will be found between the kth symbol S_k and the two neighbours S_{k-1} and

S_{k+1}, hence, we present the distance only between the kth symbol and its two nearest neighbours (see Tables VI and VII). But before that, we compute the distance between S_1 and S_2 in BPSK-CSK which is $d_b = 1.2611$. A look into Tables V, VI and VII confirm better performance of BPSK-CSK with respect to QPSK-CSK, of QPSK-CSK with respect to 8PSK-CSK and of 8PSK-CSK to 16PSK-CSK (d_b (= 1.2611) > d_q^{min} (= 0.8140) > d_8^{min} (= 0.4070) > d_{16}^{min} (= 0.2035)), d_q^{min}, d_8^{min} and d_{16}^{min} are the minimum distances in 4, 8 and 16 points constellations of MPSK-CSK, respectively.

B. Error probability

From Table VII, we can read two different values of the distance between nearest points in a 16PSK-CSK: 0.2730 and 0.2035. These distances can be expressed using d_b as 0.2730 $\approx d_b/4.62$, 0.2035 $\approx d_b/6.2$. This also applies to the height symbols constellation. We have 0.5460 $\approx d_b/2.31$ and 0.4070 $\approx d_b/3.1$. Over the QPSK-CSK constellation, we can also see that 0.8140 $\approx d_b/1.55$. Now, let us compute the error probability. We Assume that the transmission is affected by white Gaussian noise with variance given by $\sigma^2 = N_0/2$. In the case of BPSK-CSK, there is only one distance $d_b = 1.2611$ since we have 2 points. The probability of error in transmitting
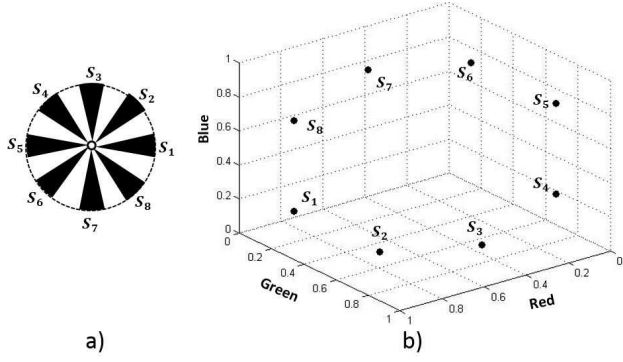
Figure 8. Representation of 8PSK complex constellation in colours for $x = 0.1331$, $V = S = 0.8533$: a) Colour wheel for 8PSK and b) the corresponding constellation in the RGB plan.
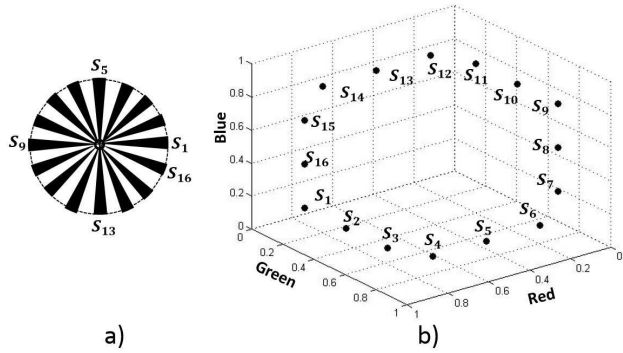

Figure 9. Representation of 16PSK complex constellation in colours for $x = 0.1331$, $V = S = 0.8533$: a) Colour wheel for 16PSK and b) the corresponding constellation in the RGB plan.

the two points is the same. The total probability P_{eB} is then given by

$$
\begin{aligned}
p_{eB} &= \frac{2}{2} \times p\left\{n > \frac{d_b}{2}\right\} \\
&= Q\left(\frac{d_b}{2\sigma}\right) \\
&= Q\left(\frac{d_b}{\sqrt{2N_0}}\right)
\end{aligned}
\tag{8}
$$

where Q(x) is given by

$$
Q(x) = \frac{1}{\sqrt{2\pi}} \int_x^\infty e^{-\frac{x^2}{2}} dx.
\tag{9}
$$

C. Simulation

Let us recall that the design must satisfy the lighting requirements while achieving communication with acceptable throughput. Firstly, we look at the HSV parameters that define the lighting. Two factors are analysed: the colour must be real and pure, which is indicated by the saturation S (see (3-b)), and it should provide enough brightness, which is calibrated by the value V (see (3-c)). We use the average value of 85.33% of $(S+V)/2$. In fact, 0.8533 is the maximum common value for V and S. This is shown in Fig. 10, where S and V are given each as a function of the parameter x. The constellation presented in Figs. 7, 8 and 9 introduced in

Table V
DISTANCES IN RGB COLOUR SPACE FOR QPSK-HSV SYMBOLS FOR $x = 0.1331$, $V = S = 0.8533$.

	s_1	s_2	s_3	s_4
s_1	0	0.8140	1.2611	0.8140
s_2	0.8140	0	0.8140	1.0298
s_3	1.2611	0.8140	0	0.8140
s_4	0.8140	1.0298	0.8140	0

Table VI
3D DISTANCES IN RGB COLOUR SPACE FOR 8PSK-CSK SYMBOLS FOR $x = 0.1331$, $V = S = 0.8533$.

s_1	s_2	s_3	s_4	s_5	s_6	s_7	s_8
s_2	s_3	s_4	s_5	s_6	s_7	s_8	s_1
0.5460	0.4070	0.4070	0.5460	0.5460	0.4070	0.4070	0.5460

Subsection IV-B, are based on 85.33% of V and S described here. Secondly, under the 85.33% condition, we analyse the HSV parameters which affect the communication performance of the system. The aim being to find the best trade-off between lighting and communication. We analyse the communication system based on different values of x that provide 85.33% average value of V and S. The simulation is divided into two parts: the first part is performed on two sets of values of the parameter x: $\mathbf{X}_1 = \{0.05, 0.075, 0.133, 0.175, 0.25\}$ and $\mathbf{X}_1' = \{1.75, 1.9, 2.1, 2.3, 2.4\}$. $\mathbf{X}_1$ and $\mathbf{X}_1'$ are chosen from either side of A and A', and correspond to the two first upper crossing point between V and S, respectively (the two first upper crossing points A and A' are shown in Fig. 10). They are chosen on the assumption that 0.79 is the threshold value of $(V + S)/2$ required to provide good lighting. Each of these sets has values of x before and after the upper crossing points (A, A'), between V and S, including the value of x on the crossing points. It is not worthy to choose values of x after the second upper crossing point A', owing to the fact that functions $V(x)$ and $S(x)$ are periodic. The system will have the same performance at $x+\Gamma$, Γ being the common period of $V(x)$ and $S(x)$. The second part of the simulation looks
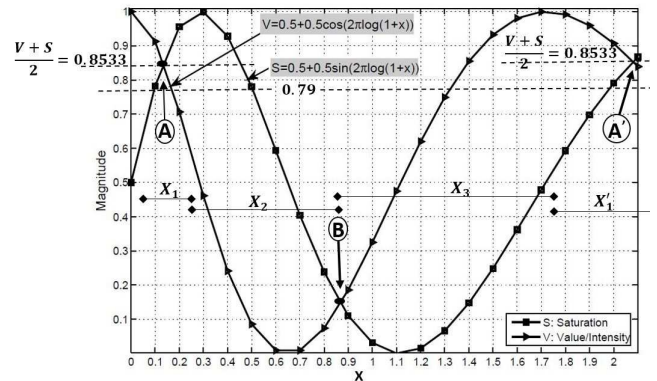

Figure 10. Variation of S and V for different values of x. We limit the range of values of x to 2 to do not reproduce the same thing. We present S and V for one period.

Table VII
3D DISTANCES IN RGB COLOUR SPACE FOR 16PSK-CSK SYMBOLS FOR
$x = 0.1331$, $V = S = 0.8533$.

s_1	s_2	s_3	s_4	s_5	s_6	s_7	s_8
s_2	s_3	s_4	s_5	s_6	s_7	s_8	s_9
0.2730	0.2730	0.2035	0.2730	0.2730	0.2035	0.2730	0.2730
s_9	s_{10}	s_{11}	s_{12}	s_{13}	s_{14}	s_{15}	s_{16}
s_{10}	s_{11}	s_{12}	s_{13}	s_{14}	s_{15}	s_{16}	s_1
0.2730	0.2730	0.2035	0.2730	0.2730	0.2035	0.2730	0.2730

Figure 11. Performance of PSK-CSK for BPSK incoming symbols: $x = 0.05$, 0.075, 0.133, 0.175, 0.25.

Figure 12. Performance of PSK-CSK for QPSK incoming symbols: $x = 0.05$, 0.075, 0.133, 0.175, 0.25.

at the performance of the communication system for values of $(V + S)/2 < 0.79$. Two sets of values of x are chosen here. $\mathbf{X}_2 = \{0.25, 0.3, 0.4, 0.65, 0.8, 0.866\}$ corresponding to the values of x before the lower crossing point and $\mathbf{X}'_2 = \{0.866, 1, 1.1, 1.5, 1.7, 1.75\}$, corresponding to the values of x after the lower crossing point (point B in Fig. 10) between V and S. We limit the analysis for the values of x from either side of only one lower crossing point for two reasons: (i) the results will be similar for other similar points, and (ii) the values of x in those sets will not be selected in the practical implementation (they produce a very low lighting with low chromaticity, hence poor performance in communication). The channel produces noise which affects the received colour c^r_k ($[c^r_{rk}, c^r_{gk}, c^r_{bk}]^T$), corresponding to the kth received symbol. c^r_k differs from the sent colour c^s_k ($[c^s_{rk}, c^s_{gk}, c^s_{bk}]^T$) and its expression is given by

$$c^r_k = \begin{cases} c^r_{rk} = c^s_{rk} + n_r \ \ (a), \\ c^r_{gk} = c^s_{gk} + n_g \ \ (b), \\ c^r_{bk} = c^s_{bk} + n_b \ \ (c), \end{cases} \tag{10}$$

where n_r, n_g and n_b are the noise affecting the RGB components of the received colour. Equation (10) is written assuming that the channel does not produce any distortion and crosstalk. In that case, the entries of the frequency response $\mathbf{H}$ (see (2)) are given by: $h_{rr} = h_{gg} = h_{bb} = 1$ (zero distortion) and $h_{ij} = 0$ for $i \neq j$ (no crosstalk). In this simulation, we also assume that $n_r = n_g = n_b = n$, with n having a Gaussian distribution with zero mean.

D. Results

We performed simulations for BPSK, QPSK, 8PSK and 16PSK incoming constellations at the input of the CSK system. This is done for different sets of values of x as indicated above in Subsection V-C. The results are shown in Figs. 11 to 26. In all cases, the results show that two important parameters influence the communication performance: x and the constellation size. In general, the performance of the system decreases as the constellation size increases. The variation of x influences the transmission. For the sets $\mathbf{X}_1$ and $\mathbf{X}'_1$, as x increases (0.05 to 0.075; 1.75 to 2.4), the performance of the system gets better for small size of constellations (BPSK-CSK and QPSK-CSK). This is not the case for 8PSK-CSK and 16PSK-CSK. For BPSK-CSK and QPSK-CSK, the best
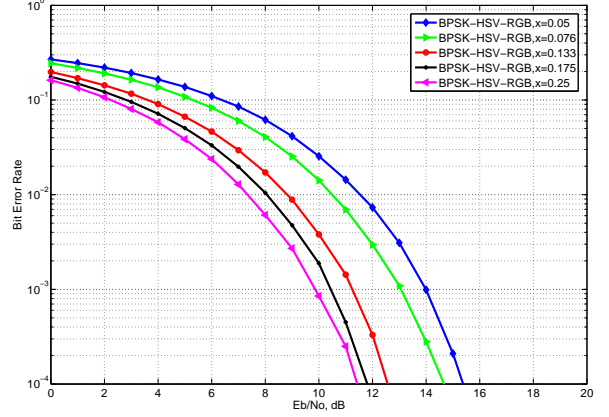
performance for the average values of $(V + S)/2$ between 79% and 85.33% is obtained for $x = \{0.25, 2.4\}$ (see Figs. 11 and 12) for the sets $\mathbf{X}_1$ and $\mathbf{X}'_1$, respectively, owing to the fact that those values of x correspond to the maximum chromaticity that the system can realise while keeping a substantial lighting (A PD is sensitive to a colour and the maximum chromaticity enables better colour detection). As the constellation size increases, we have better colour rendering but we lose in distance between point and much values of x are out of the range of good performance. We obtain the better performance of the system for $x = 0.175$ for 8PSK-CSK and 16PSK-CSK (see Figs. 13 and 14). The same logic follows Figs. 15, 16, 17 and 18 where the performance of the system is given for values of x in the sets $\mathbf{X}'_1$. At $x = 2.3$ and 2.4, the performance of the system is similar to what was obtain for $x = 0.175$ and 0.25, respectively. Note that 0.175 and 2.3 give the best performance for 8PSK-CSK and 16PSK-CSK while the best performance is obtained for BPSK-CSK and QPSK-CSK at 0.25 and 2.4.

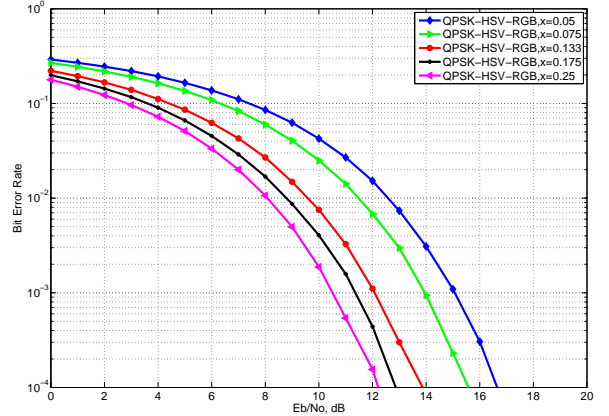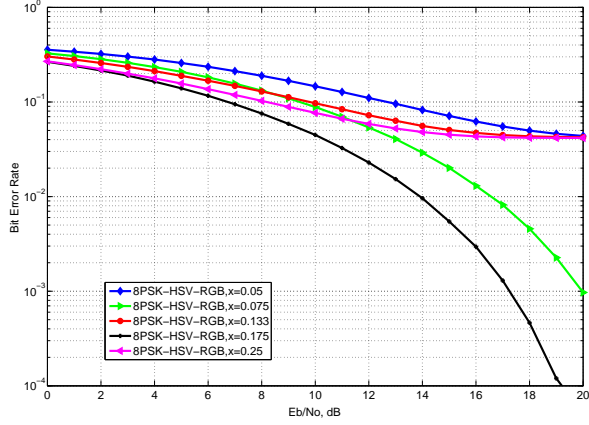Figure 13. Performance of PSK-CSK for 8PSK incoming symbols: $x = 0.05$, 0.075, 0.133, 0.175, 0.25.
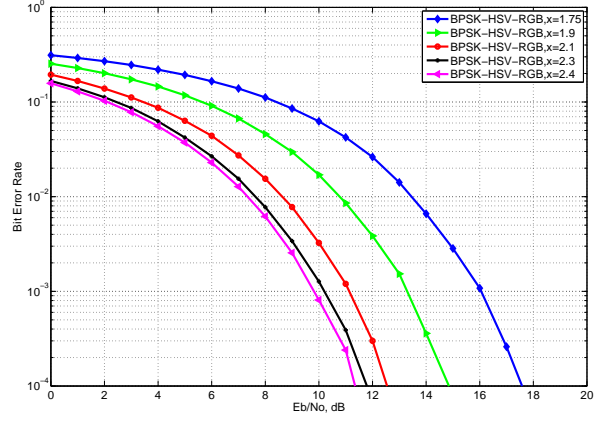

Figure 15. Performance of PSK-CSK for BPSK incoming symbols: $x = 1.75$, 1.9, 2.1, 2.3, 2.4.
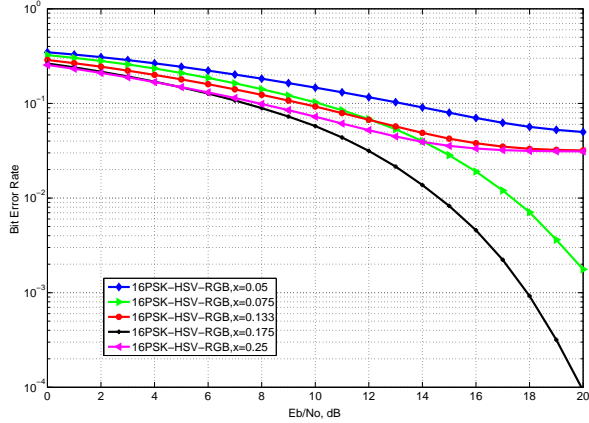

Figure 14. Performance of PSK-CSK for 16PSK incoming symbols: $x = 0.05$, 0.075, 0.133, 0.175, 0.25.
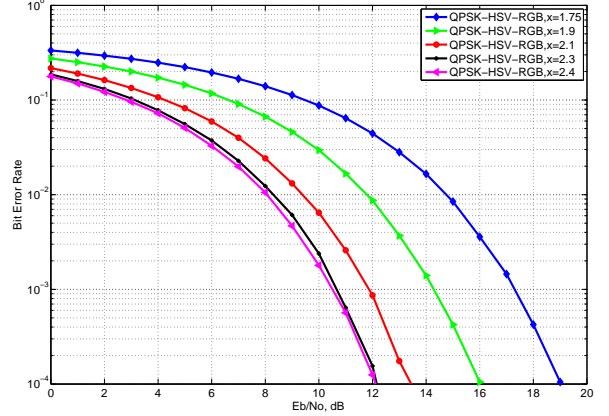

Figure 16. Performance of PSK-CSK for QPSK incoming symbols: $x = 1.75$, 1.9, 2.1, 2.3, 2.4.

The second values (2.3 and 2.4 come after one full wave of $V(x)$ and $S(x)$). Figs. 19 to 26 show the analytical results of the system performance for the values of x before and after the lower crossing (sets $\mathbf{X}_2$ and $\mathbf{X}_2'$), for all constellation sizes analysed here. Figs. 19 and 20 show that as V decreases, the performance of the system improves. As V starts to increase, the communication performance decreases, for example for the values of x between 0.65 and 0.866. For $x = 0.65$, the brightness is almost null for all colours, this explains the bad performance shown in Figs. 19 and 20 for $x = 0.65$, but the PDs can still detect substantial colours. The performances shown in Figs. 21 and 22 are quite different. This is due to the amount of colours that are transmitted. In these cases, as in any other 8 and 16 points constellation cases, the colour average is more constant. This explains why the best performance is not acceptable for $x = 0.25$. Figs. 23, 24, 25 and 26 show that for the values of x between 0.866 and 1.75, the performance of the system is poor and the worse output is obtained for $x =$

1.1, corresponding to the point where the saturation S is null. The reason of this worse performance is that the three colour receivers included in the PDs will not detect any colour, owing to the fact that the saturation is the colour term or intensity. An informed look at the results indicates that the system performs better for the values of x from either side of the upper crossing points between V and S.

VI. CONCLUSION

This paper analyses an efficient technique to map a PSK constellation to colours. The technique can be used in any hybrid system involving PSK on the first link and CSK on the second link. The system converts PSK complex constellations into colours for efficient VLC transmission. The HSV/I parameters of the colour symbols are used to create a good trade-off between communication and lighting. The requirements outlined in IEEE 802.15.7 for the power envelope and for the communication performance are both regulated by a parameter
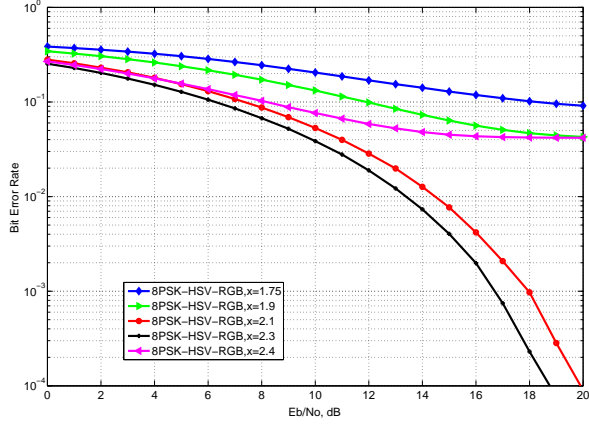
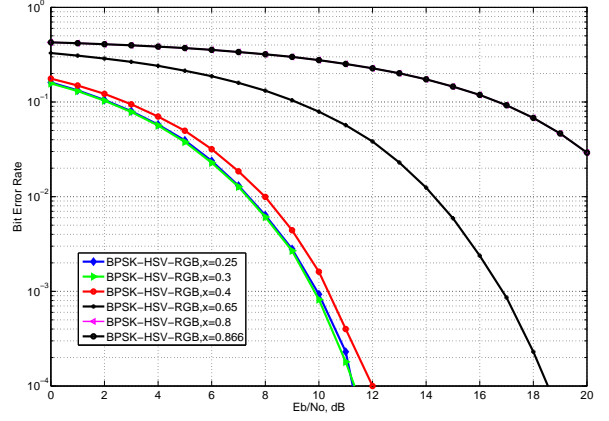Figure 17. Performance of PSK-CSK for 8PSK incoming symbols: $x = 1.75$, 1.9, 2.1, 2.3, 2.4.

Figure 19. Performance of PSK-CSK for BPSK incoming symbols: $x = 0.25$, 0.3, 0.4, 0.65, 0.8, 0.866.
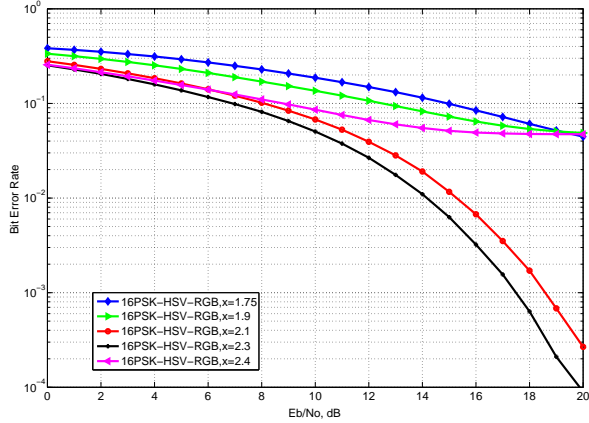

Figure 18. Performance of PSK-CSK for 16PSK incoming symbols: $x = 1.75$, 1.9, 2.1, 2.3, 2.4.
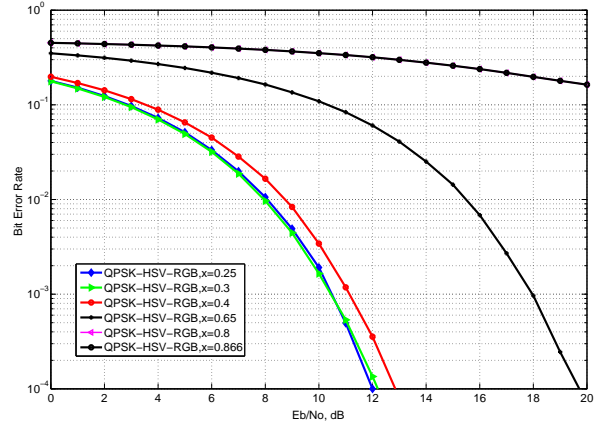

Figure 20. Performance of PSK-CSK for QPSK incoming symbols: $x = 0.25$, 0.3, 0.4, 0.65, 0.8, 0.866.

x proportional to the modulus of the PSK complex symbols. 0.8533 (85.33% of their maximum), common value of V and S, corresponding to $x = 0.1331$, provides the best performance for both communication and lighting. The selection of the optimal is based on 0.8533, value of S and V that give the best performance in lighting, it is the abscissa of point A shown in Fig. 10. Nevertheless, for a threshold of 79% taken before and after the upper crossing points between V and S, the system still gives off a substantial amount of brightness and enhances better communication throughput. The better performance in communication around four upper crossing points is obtained for the values of $x = \{0.25, 2.4\}$, corresponding to $(V + S)/2 = 0.79$ when $S > V$. The worse performance in communication is obtained for $x = 1.1$, corresponding to a saturation null. It is important to emphasize that similar conversion could be derived from quadrature amplitude modulations (QAM). 4QAM and QPSK will perform the same. From 8QAM, the lighting performance will not be met owing to the fact that the amplitude of the 8QAM symbol varies as the angle changes, this conclusion is extended to all MQAM constellations for M$\neq$4.

APPENDIX

Appendix 1: Power/colour averaging and distance optimisation in CSK design

- Power and colour averaging in CSK design

In CSK constellation design, the average power must be constant during the transmission (see Subsection IV-B). The average power, P^{avg}, is fixed by the chosen lumen value L(lm) by the relation

$$P^{avg} = \frac{L^{avg}}{\eta}, \tag{11}$$

where η is the luminous efficacy. The average luminous flux can be represented as function of the symbol and the channel gain by [17]

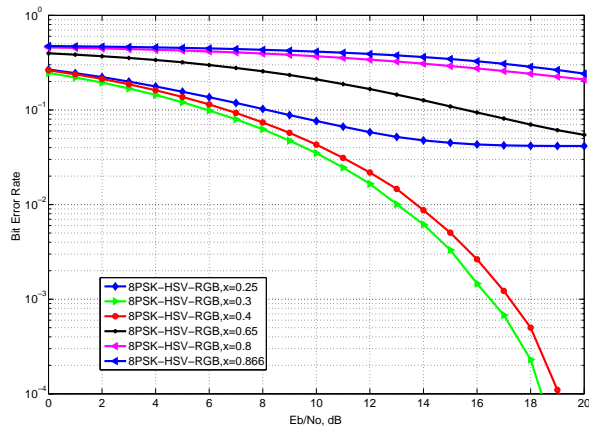$$L^{avg} = \langle \overline{g}, S_k \rangle, \tag{12}$$

Figure 21. Performance of PSK-CSK for 8PSK incoming symbols: $x = 0.25$, 0.3, 0.4, 0.65, 0.8, 0.866.
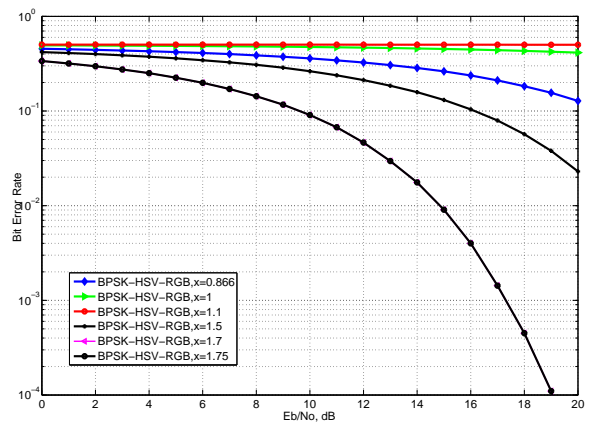

Figure 23. Performance of PSK-CSK for BPSK incoming symbols: $x = 0.866$, 1, 1.1, 1.5, 1.7, 1.75.
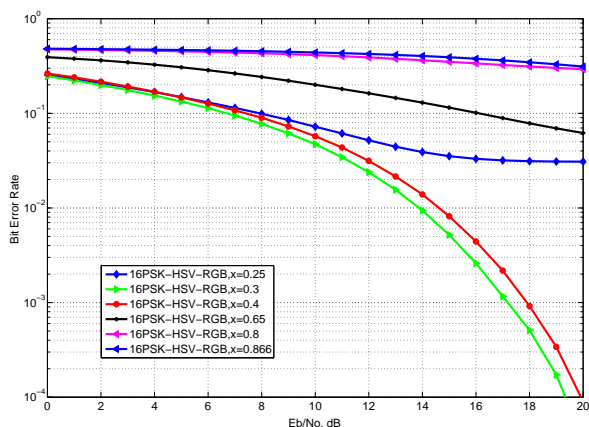

Figure 22. Performance of PSK-CSK for 16PSK incoming symbols: $x = 0.25$, 0.3, 0.4, 0.65, 0.8, 0.866.
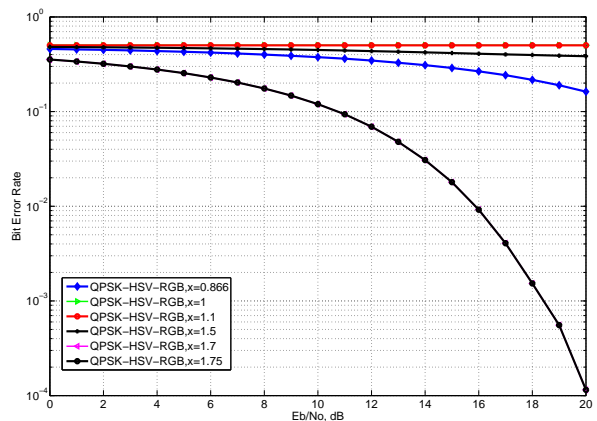

Figure 24. Performance PSK-CSK for QPSK incoming symbols: $x = 0.866$, 1, 1.1, 1.5, 1.7, 1.75.

where $\langle u, v \rangle$ is the inner product of u and v, S_k the kth symbol and $\overline{g} = [g_r, g_g, g_b]$ (g_r, g_g and g_b are the optical gain of the red, green and blue channels, respectively). The average colour is given by

$$C^{avg} = \sum_{k=1}^{N} \gamma_k S_k, \tag{13}$$

where γ_k corresponds to the probability of correctly transmitting the kth symbol. C^{avg} is defined to avoid large drift between transmitted colours.

- Probabilistic decision and distance optimisation in CSK design

The minimum square Euclidean distance target on the kth colour in CSK is given by

$$\varrho = argmin\left\{\|E_k - \mathbf{H}C_k^s\|^2\right\} \tag{14}$$

where E_k is the expected colour corresponding to the kth symbol and $\mathbf{H}$ the channel response (The other parameters are defined in the text). Note that the minimum distance between C_k^s

and C_k^r is upper-bounded by $Q[(\|E_k - \mathbf{H}C_k^s\|)/(2\sqrt{N_0/2})]$, where $(\|E_k - \mathbf{H}C_k^s\|)/2$ represents the distance from the two vectors E_k and C_k^s to the decision boundary. The objective function $\|\mathbf{e}_k - \mathbf{H}\mathbf{c}_k^s\|^2$ ($\mathbf{e}_k$ being the expectation set and $\mathbf{c}_k^s$ the transmitted set) is rearranged using a decision variable ϕ [16], [15], and the optimised detection is given by

$$\varrho = min\{\|\mathbf{e}_k(\phi) - \mathbf{H}\mathbf{c}_k^s(\phi)\|^2\}, \tag{15}$$

where $\mathbf{e}_k$ and $\mathbf{c}_k^s$ are given as function of the variable ϕ ($\mathbf{e}_k(\phi)$ and $\mathbf{c}_k^s(\phi)$). We then find a function that will meet the requirements and the constrains of the CSK constellation design. To do this, we write the distance d_{sr}:

$$d_{sr}^2 = \|C_k^r - \mathbf{H}\mathbf{c}_k^s\|^2. \tag{16}$$

Equation (16), not being differentiable, needs to be approximated [16], [15]. We find a function that approximates (16) and satisfies (14). The following objective function (17)
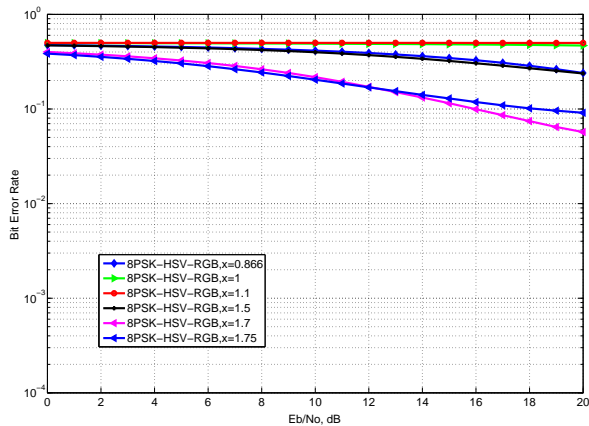
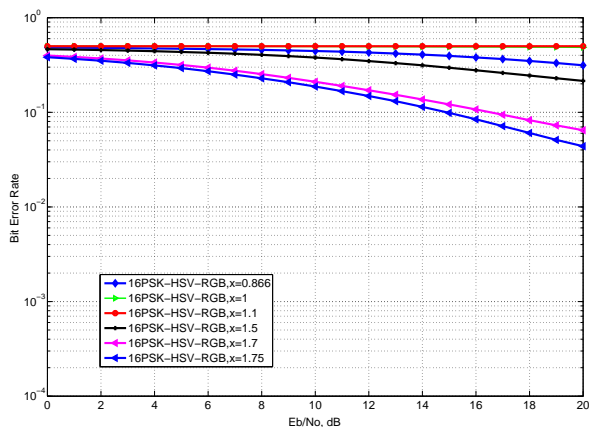Figure 25. Performance of PSK-CSK for 8PSK incoming symbols: $x = 0.866$, 1, 1.1, 1.5,1.7, 1.75.

Figure 26. Performance PSK-CSK for 16PSK incoming symbols: $x = 0.866$, 1, 1.1, 1.5,1.7, 1.75.

preferably represents the above described objective detection situation [16], [15], and [25].

$$\frac{ln}{\beta} \sum_{r \neq s} exp(-\beta \|E_k - \mathbf{H}C_k^s\|^2) \qquad (17)$$

The solution $f(\phi)$ given in (18), which is a function of the decision variable ϕ satisfies the maximum detection probability (14) [15].

$$f(\phi) = \frac{ln}{\beta} \sum_{e \neq s} exp(-\beta \|\mathbf{e}_k(\phi) - \mathbf{H}c_k^s(\phi)\|^2) \qquad (18)$$

REFERENCES

[1] Ieee standard for local and metropolitan area networks–part 15.7: Short-range wireless optical communication using visible light," IEEE Std 802.15.7-2011, pp. 1–309, Sep. 2011

[2] Roberts, R.D.; Rajagopal, S.; Sang-Kyu Lim, "IEEE 802.15.7 physical layer summary," IEEE GLOBECOM Workshops (GC Wkshps), pp. 772-776, 5-9 Dec. 2011, Houston, Texas, USA.

[3] A. R. ndjiongue, H. C. ferreira, and T. M. N. Ngatched, "Visible light communications (vlc) technology," in Wiley Encyclopedia of Electrical and Electronics Engineering, C. Strickland, Ed. 15 Jun., pp. 1-15, John Wiley and Sons.

[4] Li, Xuan, Rong Zhang, and Lajos Hanzo. "Cooperative load balancing in hybrid visible light communications and WiFi." IEEE Transactions on Communications, vol. 63, n°. 4, pp. 1319-1329, Apr. 2015.

[5] Jian Song, Wenbo Ding, Fang Yang, Hui Yang, Bingyan Yu and Hong-ming Zhang. "An Indoor Broadband Broadcasting System Based on PLC and VLC." IEEE Transactions on Broadcasting, vol. 61, n°. 2, pp.299-308, Jun. 2015.

[6] Ding, Wenbo, Fang Yang, Hui Yang, Jintao Wang, Xiaofei Wang, Xun Zhang, and Jian Song. "A hybrid power line and visible light communication system for indoor hospital applications." Computers in Industry 68, pp. 170-178, 2015.

[7] Komine, Toshihiko, and Masao Nakagawa. "Integrated system of white LED visible-light communication and power-line communication." IEEE Transactions on Consumer Electronics, vol. 49, n°. 1, pp. 71-79, Jun. 2003.

[8] A. R. Ndjiongue, Thokozani Shongwe, H. C. Ferreira, T. M. Nkouatchah Ngatched and A. J. Han Vinck, "Cascaded PLC-VLC Channel Using OFDM and CSK Techniques", IEEE Global Communications Conference (GLOBECOM), Dec. 6-10 2015, San Diego, CA, USA.

[9] A. R. Ndjiongue, Hendrik C. Ferreira, K. Ouahada, and A. J. Vinck. "Low-complexity SOCPBFSK-OOK interface between PLC and VLC channels for low data rate transmission applications." 18th IEEE International Symposium on Power Line Communications and its Applications (ISPLC), pp. 226-231, Mar. 30 - Apr. 2, 2014, Glasgow, Scotland, UK.

[10] A. D. Familua, A. R. Ndjiongue, K. Ogunyanda, L. Cheng, H. C. Ferreira, T. G. Swart, "A Semi-hidden Markov modeling of a low complexity FSK-OOK in-house PLC and VLC integration," IEEE International Symposium on Power Line Communications and its Applications (ISPLC), pp.199-204, Mar. 29 2015-Apr. 1 2015, Texas, USA.

[11] Rahaim, Michael B., Anna Maria Vegni, and Thomas DC Little. "A hybrid radio frequency and broadcast visible light communication system." IEEE GLOBECOM Workshops (GC Wkshps), pp. 792-796, Houston, Texas, USA.

[12] S. Pergoloni, M. Biagi, S. Rinauro, S. Colonnese, R. Cusani, G. Scarano, "Merging Color Shift Keying and Complementary Pulse Position Modulation for Visible Light Illumination and Communication," Journal of Lightwave Technology, vol. 33, n°. 1, pp. 192-200, Jan. 1 2015.

[13] J. M. Luna-Rivera, R. Perez-Jimenez, V. Guerra-Yañez, C. Suarez-Rodriguez, F. A. Delgado-Rajo, "Combined CSK and pulse position modulation scheme for indoor visible light communications," Electronics Letters , vol. 50, n°. 10, pp.762-764, May 2014.

[14] E. Monteiro, S. Hranilovic, "Constellation design for color-shift keying using interior point methods," IEEE GLOBECOM Workshops (GC Wkshps), pp. 1224-1228, 3-7 Dec. 2012, Anaheim, CA, USA.

[15] R. J. Drost, B. M. Sadler, "Constellation Design for Channel Precompensation in Multi-Wavelength Visible Light Communications," IEEE Transactions on Communications, vol. 62, n°. 6, pp. 1995-2005, Jun. 2014.

[16] R. J. Drost, B. M. Sadler, "Constellation design for color-shift keying using billiards algorithms," IEEE GLOBECOM Workshops (GC Wkshps), pp. 980-984, 6-10 Dec. 2010, MIAMI, FLORIDA, USA.

[17] E. Monteiro, S. Hranilovic, "Design and Implementation of Color-Shift Keying for Visible Light Communications," Journal of Lightwave Technology, vol. 32, n°. 10, pp. 2053-2060, May 2014.

[18] P. Ganesan and V. Rajini. "Value based semi automatic segmentation of satellite images using HSV color space, histogram equalization and modified FCM clustering algorithm." IEEE International Conference on Green Computing, Communication and Conservation of Energy (ICGCE), pp. 77-82., 12-14 Dec. 2013, Chennai.

[19] A. W. M. Smeulders, M. Worring, S. Santini, A. Gupta, R. Jain, "Content-based image retrieval at the end of the early years," IEEE Transactions on Pattern Analysis and Machine Intelligence, vol. 22, n°. 12, pp. 1349-1380, Dec 2000.

[20] Farris, Frank A. "Visualizing complex-valued functions in the plane." AMC 10 1997.

[21] Conway, John B. Functions of One Complex Variable II: II. vol. 2. Springer Science and Business Media, 1995.

[22] S. Rajagopal, R. D. Roberts, Sang-Kyu Lim, "IEEE 802.15.7 visible light communication: modulation schemes and dimming support," IEEE Communications Magazine, vol. 50, n°. 3, pp. 72-82, Mar. 2012.

[23] Wade, Lawrence A. "An evanescent perspective on cells." PhD diss., California Institute of Technology, 2011.

[24] Ibraheem, A. Noor, M. Mokhtar Hasan, Rafiqul Z. Khan, and Pramod K. Mishra. "Understanding color models: a review." ARPN Journal of Science and Technology, vol. 2, n°. 3, pp. 265-275, 2012.

[25] Mingxuan Zhang; Zaichen Zhang, "Fractionally spaced equalization in visible light communication," IEEE Wireless Communications and Networking Conference (WCNC), pp. 4282-4287, 7-10 Apr. 2013, Shanghai.